EUROPEAN ORGANIZATION FOR NUCLEAR RESEARCH

Proposal to the ISOLDE and Neutron Time-of-Flight Committee

(Following HIE-ISOLDE Letter of Intent I-224)

Probing the fission and radiative decay of the ^{235}U+n system using (d,pf) and (d,$p\gamma$) reactions

January 11, 2023

S. A. Bennett[1], D. K. Sharp[1], T. Wright[1], M. Au[2], P. A. Butler[3], A. Camaiani[4], D. J. Clarke[1], A. J. Dolan[3], S. J. Freeman[1,2], L. P. Gaffney[3], K. Garrett[1], S. A. Giuliani[5], A. Heinz[6], H. T. Johansson[6], B. R. Jones[3], B. Jonson[6], A. Kawecka[6], B. P. Kay[7], J. Klimo[4], M. Kowalska[2,8], M. Labiche[9], I. Lazarus[9], P. T. MacGregor[2], B. Marsh[2], M. Managlia[6], G. Martínez-Pinedo[10], T. Nilsson[6], J. Ojala[3], B. Olaizola[2], R. D. Page[3], O. Poleshchuk[4], R. Raabe[4], S. Reeve[1], B. Reich[2], A. Rodriguez[2], S. Rothe[2] and A. G. Smith[1], H. Törnqvist[6], A. Youssef[4].

[1]*School of Physics and Astronomy, The University of Manchester, Manchester M13 9PL, UK*
[2]*ISOLDE, CERN, CH-1211 Geneva 23, Switzerland*
[3]*Oliver Lodge Laboratory, University of Liverpool, Liverpool, L69 7ZE, UK*
[4]*KU Leuven, Instituut voor Kern- en Stralingsfysica, 3001 Leuven, Belgium*
[5]*Department of Theoretical Physics, Universidad Autónoma de Madrid, 28049 Madrid, Spain*
[6]*Institutionen för Fysik, Chalmers Tekniska Högskola, S-412 96 Göteborg, Sweden*
[7]*Physics Division, Argonne National Laboratory, Argonne, Illinois 60439, USA*
[8]*University of Geneva, Geneva, Switzerland*
[9]*STFC Daresbury Laboratory, Daresbury, Warrington, WA4 4AD, UK*
[10]*Institut für Kernphysik, Technische Universität Darmstadt, Germany*

Spokespersons: Sam Bennett (samuel.bennett@manchester.ac.uk), David Sharp (david.sharp@manchester.ac.uk) and Toby Wright (tobias.wright@manchester.ac.uk)
ISOLDE contact: Patrick MacGregor (patrick.macgregor@cern.ch)

CERN-INTC-2023-019 / INTC-P-659
11/01/2023

Abstract: We propose a simultaneous measurement of the ^{235}U(d,pf) and ^{235}U(d,$p\gamma$) reactions in inverse kinematics with the ISOLDE Solenoidal Spectrometer. The aim of the measurement is to simultaneously deduce the fission and radiative decay probabilities. This measurement shall facilitate the development of a new technique that will enable access to fission data for short-lived systems. These data are important for fission contributions to the astrophysical r-process, fundamental understanding of fission as well as terrestrial applications. We propose a winter physics measurement in order to commission a new experimental configuration at ISS, combining the standard ISS setup with a recently constructed fission array, and gamma-ray scintillator array.

Requested shifts: 20 shifts, split into 1 run over 1 year (winter running period).
Installation: ISOLDE Solenoidal Spectrometer

1 Physics case

Studying the process of nuclear fission offers fundamental information required to both validate and further develop reliable nuclear models, whilst also providing crucial data for a wide range of fields including nuclear astrophysics, basic research, and applications such as nuclear energy, security, safeguards and isotope production [1]. Despite fission being discovered over 80 years ago, this complex process still presents challenges for both experimentalists, studying fissioning systems, and theorists alike, aiming to produce robust and predictable descriptions of the fission process. An opportunity exists to extend the scope of current fission studies, by combining the potential availability of actinide beams at HIE-ISOLDE with the implementation of a fission detection setup with the ISS.

Measurements of fission cross sections, fission-fragment yield distributions and barrier heights collectively provide fundamental information on the fission process [2]. In particular, whilst direct measurements of fission barriers and angular momentum distributions are experimentally challenging, they are important components in understanding the fission process [5, 6, 7, 8]. These observables are also inputs into state-of-the-art nucleosynthesis calculations for the astrophysical r-process and the related fission recycling processes [3, 4]. Moreover, these data are critical in the design of advanced nuclear reactors and waste transmutation in sub-critical reactors [2].

The study of neutron-induced fission by direct neutron irradiation is possible only in a limited subset of nuclei close to stability. For example, many fission cross section measurements have been performed at the n_TOF facility [9] from thermal up to GeV incident neutron energies. Experiments are however limited by target properties and availability; aside from access to enriched material, both the natural radioactivity and diminishing lifetimes of ever more exotic desired isotopes make fixed target experiments unfeasible. Additionally, direct measurement of the fission barrier height in fissile isotopes is not possible using neutron induced reactions. Charged particle and photon-induced fission have been studied [5, 6, 7] but these measurements exist only for isolated stable or long-lived isotopes [5, 6]. Measurements have generally focused on extracting one experimental parameter rather than using one data set to determine several — it is advantageous to determine fission parameters simultaneously using multi-modal detection and under selectable experimental conditions. Moreover, the range of available excitation energies of the compound nucleus prior to fission is often restricted [6] and often not well defined in a particular experiment. Recent measurements with radioactive ion beams have used beta-delayed fission to measure barrier heights; these results exhibit discrepancies between 15% and 40% with respect to theoretical calculations [8]. To overcome these issues, experimental techniques that directly probe the aforementioned fission properties are required.

Using radioactive ion beams in inverse kinematics offers a way of achieving multi-modal detection of fission observables in exotic fissioning systems with a number of advantages. By passing the radioactive ion beam through a deuterated CD_2 target and using the single-neutron-adding (d,p) reaction (see Ref. [10] for example), compound nucleus states across a wide range of excitation energy can be populated, both above and below the fission barrier and neutron separation energy, S_N. Direct measurement of this excitation energy through the kinematics of the ejected proton and observation of the fission fragments gives the fission probability as a function of excitation energy, in the regions above and below both the fission barrier and S_N simultaneously, in a way not currently possible with other techniques. This technique therefore

provides a direct measurement of the fission barrier height. The use of inverse kinematics provides further advantages. Light-mass target contamination can limit (d, pf) measurements in normal kinematics to low energies [2, 11, 12]; using an actinide beam in inverse kinematics can address this problem. The solenoidal spectrometer technique allows the (d, pf) reaction to be well separated from other potential transfer and fusion evaporation reaction channels involving the carbon in the target — at the beam energies of several MeV/nucleon required for the transfer reaction, reaction products from these channels are predominantly forwards focused, whilst protons from the (d, p) reaction are emitted into the backwards hemisphere.

Finally, recent theoretical work has demonstrated a strong sensitivity of the fission probability to the angular momentum of the fissioning state [13, 14], especially pronounced around fission thresholds; it may be possible to shed light on the role of angular momentum in the fission process by measuring the average angular distribution of the ejected protons in the centre-of-mass frame, which is related to the angular momentum distribution of the populated states that subsequently lead to fission. It is well known that there can be large discrepancies when using the 'surrogate' methodology to study neutron capture [15], much more so than for the case of fission. This is largely driven by strong sensitivity of neutron emission to the spin of the decaying nucleus, especially near S_N, with the spins populated in neutron induced and direct reactions being quite different. There have however been significant improvements, largely theoretical, made to the technique in recent years, see for example Ref. [16, 17]. By simultaneously studying both the fission and radiative decay channels, and with access to the angular momentum transferred to the decaying system, experiments such as the one we propose may help to elucidate this issue.

A proof-of-principle fission measurement was made in early 2020, using a setup similar to that described in Section 2, to test and verify the technique with HELIOS at Argonne National Laboratory (ANL). The test case was the ^{238}U(d,pf) reaction, using which the fission barrier height of ^{239}U was extracted and compared well to the existing value, as shown in Fig. A4. It is expected that with future upgrades to the ISS hardware and the fission detectors described below, cases with significantly lower event rates will be made feasible, allowing the measurement of more exotic fissioning systems. Furthermore there is ongoing work to improve the extraction of actinides from primary targets which will further facilitate such measurements, see for example Ref. [18].

2 Experimental details

Reaction and beam energy— We propose to use single neutron transfer reactions to populate excited states in ^{236}U in order to obtain the respective fission and radiative capture probabilities as a function of excitation energy. This shall be achieved by studying the (d,pf) and $(d,p\gamma)$ reactions in inverse kinematics, with an incident ^{235}U beam energy of 7 MeV/nucleon. This reaction is an ideal commissioning case, where beam rates are relatively high (see below), and where the capability to study the competition between fission and radiative capture and measure their relative probabilities below S_N can be demonstrated. The highest available beam energy is required to maximise the (d,p) cross section. Maximising the incident beam energy also leads to a more forward peaked (d,p) proton angular distribution in the centre-of-mass (c.m.) frame with respect to the beam direction, and to a more backward peaked distribution in the laboratory. This provides a larger (d,p) geometrical detection efficiency and therefore a larger measured rate of (d,pf) events, also covering a larger range of possible ℓ transfers in the

(d,p) reaction.

Experimental set-up— A schematic of the set-up and example kinematics is shown in Fig. 1. We intend to use the ISS installation with the Liverpool silicon array in combination with an array of heavy-ion gas filled fission detectors developed at Manchester, and the Leuven $CeBr_3$ scintillator array. The fission detectors, shown in Fig. A1, were proven to function well with HELIOS at ANL during the $^{238}U(d,pf)$ reaction measurement [19], and the $CeBr_3$ infrastructure, shown in Fig. A2, was demonstrated for use with ISS in November 2022.

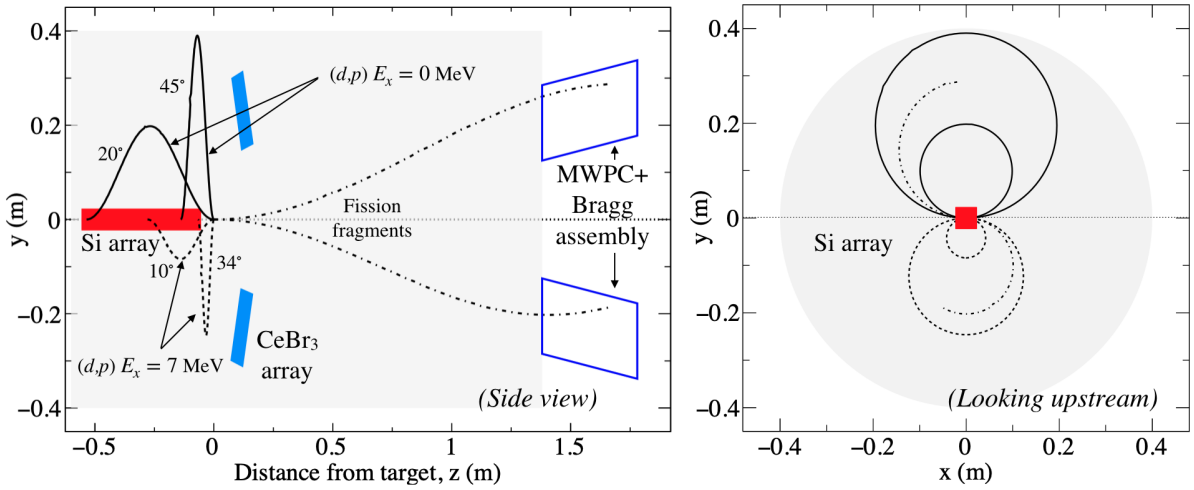

Figure 1: Schematic of the experimental setup with example particle trajectories, for states populated above and below the fission barrier, for $^{235}U(d,pf)$ at 7 MeV/nucleon. The inside of the ISS vessel is represented by the grey shaded regions.

In inverse kinematics, a heavy beam is incident on a deuterated polyethylene (CD_2) target. Protons from (d,p) reactions are emitted into the backward hemisphere with respect to the beam direction. The Liverpool silicon array with the end placed 55 mm upstream of the target shall be used to momentum analyse the outgoing protons from (d,p) reactions leading to excited ^{236}U residual nuclei. With ISS, targets with thicknesses $\approx$ 100 $\mu g/cm^2$ allow the reaction Q value to be determined with a resolution of around 120 keV. Whilst a minimal Q-value resolution is critical for spectroscopic experiments, for the case of these proposed measurements where the level density is too high for state-by-state analysis, a Q-value resolution of several hundred keV is acceptable. This is because the fission and capture probabilities typically vary over a scale of several hundreds of keV in excitation energy around the first chance fission threshold. For example, in the $^{238}U(d,pf)$ commissioning experiment at HELIOS, targets with thicknesses $\approx$ 400-500 $\mu g/cm^2$ were used in order to maximise statistics. The associated Q-value resolution was estimated to be around 300 keV FWHM. There is therefore scope to increase the target thickness further to gain greater statistics. To mitigate against the effect of target degradation with beam dose, we intend to use an array of 64 targets.

The in-flight fission of residual nuclei leads to a strongly forward peaked fission fragment distribution downstream of the target in the laboratory, shown in Fig. A3; fragments emitted over

4π in the c.m. are boosted into a relatively small solid angle in the lab ($\theta_{lab} \lesssim 20^\circ$ - dependent on beam energy). Four arms each comprising of a position sensitive multi-wire proportional counter (MWPC) and axially segmented Bragg detector are equally spaced in the azimuthal direction, shown in Fig. A1. The opening apertures to the ISS vacuum vessel are positioned at a radial distance of 21.5 cm from the beam axis, and the arms are oriented at angles of 12° with respect to the beam axis. With this arrangement, the c.m. fission axis angular coverage for given mass splits is shown in Fig. A3. The total geometric fission fragment detection efficiencies, for both coincident light and heavy and non-coincident events, are given in Table 1.

The MWPCs, operated with C_3F_8 at a pressure of 8 mbar, provide a precise time reference with a resolution of < 10 ns for correlating fission events with Si array events, in addition to providing the position of fragments at the entrances to the Bragg detectors, operated with CF_4 at a pressure of 400 mbar. The kinetic energy and specific energy-loss of fission fragments ($\mathrm{d}E/\mathrm{d}x$) are measured with the Bragg detectors, via digital pulse shape analysis. Physics events will be defined by the detection of a proton in the on-axis silicon array, and the subsequent decay channel can be selected by gating on events in either the fission or scintillator detectors.

Absolute cross sections will be extracted by monitoring the target thickness via elastically-scattered deuterons detected with an annular silicon monitor detector positioned 0.3 m downstream of the target.

Fission barrier and probability— By gating on (d,pf) events, one can select fission events, and the fission probability P_f is defined as

$$P_f(E_{ex}) = \frac{N_{d,pf}(E_{ex})}{\epsilon_f N_{d,p}(E_{ex})}, \tag{1}$$

where $N_{d,p}$ and $N_{d,pf}$ are the numbers of (d,p) singles and (d,pf) events respectively, and ϵ_f is the fission detection efficiency derived from a Monte-Carlo simulation. At and above the fission barrier, a sharp increase in fission-fragment yields occurs. The counts N and fission probability deduced in the ^{238}U(d,pf) test case are shown in Figure A4.

Radiative capture probability— By gating on (d,$p\gamma$) events, one can select the radiative capture channel, assuming that the residual nucleus always proceeds through a compound state (also assumed in the Oslo method, see for example Ref. [22]) [16, 17]. Similar to the fission probability, the capture probability as a function of excitation energy E_x is given by

$$P_\gamma(E_x) = \frac{N_{d,p\gamma}(E_x)}{\epsilon_\gamma N_{d,p}(E_x)}. \tag{2}$$

In this case however, one needs to use the total energy detection method (TED) since the gamma ray detection array coverage is $\ll 4\pi$. By applying the pulse-height weighting technique (PHWT), the number of (d,$p\gamma$) events can be deduced [23]. A 'weighting function' $W(E_d)$, where E_d is the measured deposited energy, is applied to the experimental data on an event-by-event basis, artificially modifying the detection efficiency ϵ_γ such that it becomes proportional to the gamma ray energy. In this case, the capture probability is given by

$$P_\gamma(E_x) = \frac{N_{d,p\gamma}(E_x)}{\epsilon_\gamma N_{d,p}(E_x)} = \frac{\sum_{E_d} N_{d,p\gamma}(E_x, E_d) W(E_d)}{N_{d,p}(E_x) \sum_{E_d} W(E_d)}. \tag{3}$$

Prompt fission gamma rays originating from events in which fission fragments are not detected will inevitably contribute to scintillator array - Si array coincident events, $N_{d,p\gamma}(E_x)$. This contribution shall be evaluated and subtracted by using the measured prompt fission gamma ray spectrum (see below), and knowledge of the fission detection efficiency.

Fission A- and Z-yields— Mass split has been determined with approximately 10 amu resolution for the case of ^{238}U(d,pf) with HELIOS. Analysis for the extraction of Z-yields is still underway, but in principle the atomic number of fragments can be determined with Bragg peak spectroscopy [24].

Prompt fission gamma ray spectra (PFGS)— Of interest in nuclear power generation is reactor heating caused by prompt fission gamma rays. In these studies, the presence of the scintillator array will allow a measurement of the PFGS, by making Si array - fission MWPC - scintillator array coincidences.

Background reactions— The impact of light ion reaction products was already discussed in Section 1. Reactions of the beam on the carbon in the CD_2 targets can lead to multinucleon transfer, where reaction products travel into the backwards hemisphere, followed by fission [25]. It was found for ^{238}U(d,pf) that the fission - Si array coincidence rate from carbon induced reactions was around 3-4$\times$ larger than the (d,pf) rate around the fission barrier. This source of background was addressed by taking data with a pure $^{\rm nat}$C target; around 46% of data taking time should be spent on measuring with the C targets for optimal counting errors in background subtracted spectra (for the same CD_2 and $^{\rm nat}$C target areal densities). A second source of background arises from deuteron breakup, whereby the measurement of protons from such reactions detected with the Si array contribute to the (d,p) singles ($N_{d,p}$ in Equations 1 and 2) leading to an underestimate of the decay probability, typically by around 10% [26]. This effect can be calculated in order to correct the experimental data, see for example Ref. [26]. Correction calculations for the case of our ^{238}U(d,pf) measurement are underway [27]. A potential source of background when performing the capture probability are neutrons detected with the scintillator array. Prompt fission neutrons from fission events that go undetected have energies around 1 MeV/nucleon, and are therefore boosted forwards in the laboratory at roughly the same angle as the fission fragments, thereby reducing their impact as a source of background.

HIE-ISOLDE technical considerations— It is intended that the measurement would be performed as a winter physics campaign. Time averaged beam rate at ISS is envisaged to be around 2.5×10^5 pps, assuming the transmission efficiency through HIE-ISOLDE is around 5%, and where the out-of-target rate is estimated to be around 5×10^6 pps. It is expected that the maximum attainable beam energy will be around 7 MeV/nucleon. We would expect some level of ^{238}U contamination given the use of a UC_x primary target. Even with significant contamination, the extraction of the fission barrier in ^{236}U shall not be affected significantly since in ^{236}U it is around 0.5 MeV lower than that of ^{239}U.

Due to the relatively large EBIS charge breeding time for the proposed isotope, a low duty cycle will be required, leading to a beam repetition rate as low as 0.2 s^{-1}. The instantaneous detector rates could be up to 5000 times larger than the time averaged rates. Estimates of the instantaneous rates in the Si array and fission detectors are given in Table 1, and are within

the respective operating capabilities.

Beam time request— We request 20 shifts of offline beam time delivering ^{235}U at an energy of $\geq$7 MeV/nucleon: 10 shifts for data taking with CD_2 targets, 9 shifts with ^{nat}C targets, and 1 shift for optimising beam delivery to ISS. The expected experimental counting rates are given in Table 1. The projected yields are based on the ^{238}U(d,pf) HELIOS experiment performed at 8.6 MeV/nucleon. Calculating such reaction rates is a non-trivial task due to the large number of participating states populated in the transfer reaction, and the sensitivity of the fission probability to the spin of each state. DWBA calculations, using the code Ptolemy, suggest that there will be a reduction of between 10-20% to the (d,p) cross section for ^{235}U(d,p) at 7 MeV/nucleon compared to ^{238}U(d,p) at 8.6 MeV/nucleon, depending on the ℓ transfer. It is assumed that the probability of compound nucleus formation after populating doorway states with the direct reaction does not vary significantly between the proposed case and the previously measured case. Here, a slightly lower magnetic field strength compared to the HELIOS experiment will extend the angular coverage of the Si array, increasing the solid angle coverage where the (d,p) cross section is larger (all ℓ transfers peak between around 40° and 60°). Based on these assumptions, we would expect a total of around 1500 (d,pf) events, allowing the fission probability above the fission barrier to be defined with an uncertainty of $< 10\%$ with 200 keV bins.

	^{235}U at 7 MeV/u	^{238}U at 8.6 MeV/u
Beam mode	Offline	—
Central magnetic field strength	2.3 T	2.5 T
Fission probability at 1st chance	0.68	0.19
Total fission detection efficiency	0.37	0.31
Coincident fission detection efficiency	0.015	0.065
$CeBr_3$ γ detection efficiency at 1 MeV	2.5%	—
Si array to CD_2 target distance	55 mm	55 mm
Si array c.m. angular coverage at $E_x = 0$ MeV	$20° \rightarrow 45°$	$25° \rightarrow 46°$
Si array c.m. angular coverage at $E_x = 7$ MeV	$10° \rightarrow 34°$	$9° \rightarrow 31°$
Si array azimuthal angular coverage	70%	45%
Beam intensity (out of UC_x target)	5×10^6 pps	—
Beam intensity (at experiment)	2.5×10^5 pps	$\approx 10^6$ pps
Proposed shifts CD_2 target (0.5 mg/cm^2)	10	—
Proposed shifts C target (0.5 mg/cm^2)	9	—
Measured (d,p) events	6.1×10^5	3.5×10^5
Measured (d,pf) events (singles efficiency)	1.5×10^3	840
Measured (d,$p\gamma$) events	~ 1000	—
Si array instantaneous rate	1.7×10^4 s^{-1}	—
Fission detectors instantaneous rate	300 s^{-1}	—

Table 1: Experimental parameters, and estimates of expected count rates projected from the case of the ^{238}U(d,pf) measurement with HELIOS. 'Total' and 'coincident' fission detection efficiency refers to the detection of ≥ 1 fragment, and 2 fragments, respectively.

Summary of requested shifts: We request a total of **20 shifts** during the winter physics period, with a beam of ^{235}U at an energy of $\geq$7 MeV/nucleon.

References

[1] Nuclear Data Needs and Capabilities for Applications, May 27-29, 2015, Lawrence Berkeley National Laboratory, Berkeley CA, arXiv:1511.07772.

[2] J. E. Escher, *et al.*, Rev. Mod. Phys. **84**, 353 (2012).

[3] I. V. Panov, *et al.*, Nucl. Phys. A **747**, 633 (2005).

[4] M. R. Mumpower, *et al.*, Prog. Part. Nucl. Phys. **86**, 86 (2016).

[5] A. N. Andreyev, *et al.*, Rep. Prog. Phys. **81**, 016301 (2018).

[6] K.-H. Schmidt and B. Jurado, Rep. Prog. Phys. **81**, 106301 (2018).

[7] S. Kailas and K. Mahata, Pramana **83** 851 (2014).

[8] M. Veselsky, *et al.*, Phys. Rev. C **86**, 024308 (2012).

[9] N. Colonna, *et al*, Eur. Phys. J. A **56**, 48 (2020).

[10] Q. Ducasse, *et al.*, Phys. Rev. C **94**, 024614 (2016).

[11] E. F. Lyles, *et al.*, Phys. Rev. C **76**, 014606 (2007).

[12] C. Rodriguez-Tajes, *et al.*, Phys. Rev. C **89**, 024614 (2014).

[13] J. E. Escher and F. S. Dietrich, Phys. Rev. C. **74**, 054601 (2006).

[14] S. Chiba and O. Iwamoto, Phys. Rev. C. **81**, 044604 (2010).

[15] G. Boutoux, *et al.*, Phys. Lett. B. **712**, 319–325 (2012).

[16] A. Ratkiewicz, *et al.*, Phys. Rev. Lett. **122**, 052502 (2019).

[17] J. E. Escher, *et al.*, Phys. Rev. Lett. **121**, 052501 (2018).

[18] M. Au *et al.*, CERN-INTC-2022-028 / INTC-I-243 13/05/2022.

[19] S. A. Bennett, *et al.*, Submitted to PRL November 2022.

[20] K.-H. Schmidt, *et al.*, Nuclear Data Sheets **131**, 107 (2016).

[21] S. Bjørnholm and J. E. Lynn, Rev. Mod. Phys. **52**, 725 (1980).

[22] F. Zeiser, *et al.*, Phys. Rev. C **100**, 024305 (2019).

[23] U. Abbondanno, *et al.*, Nucl. Instr. Meth. **521**, 454 (2004).

[24] C. R. Gruhn, *et al.*, Nucl. Instrum. Methods **196**, 33 (1982).

[25] M. Caamaño, *et al.*, Phys. Rev. C **88**, 024605 (2013).

[26] Q. Ducasse, *et al.*, Phys. Rev. C **94**, 024614 (2016).

[27] J. Escher and G. Potel, Private Communication.

Appendix A

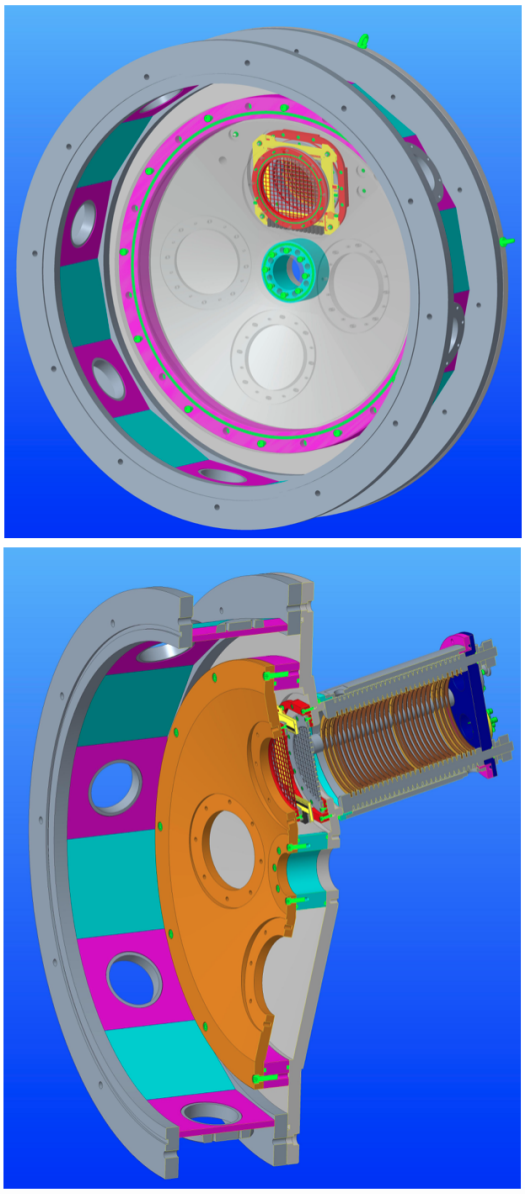

Figure A1: Drawings showing the arrangement of the existing fission detectors to be attached to the newly manufactured downstream door of ISS. The entrances to the detectors are situated 1.38 m from the CD_2 target.

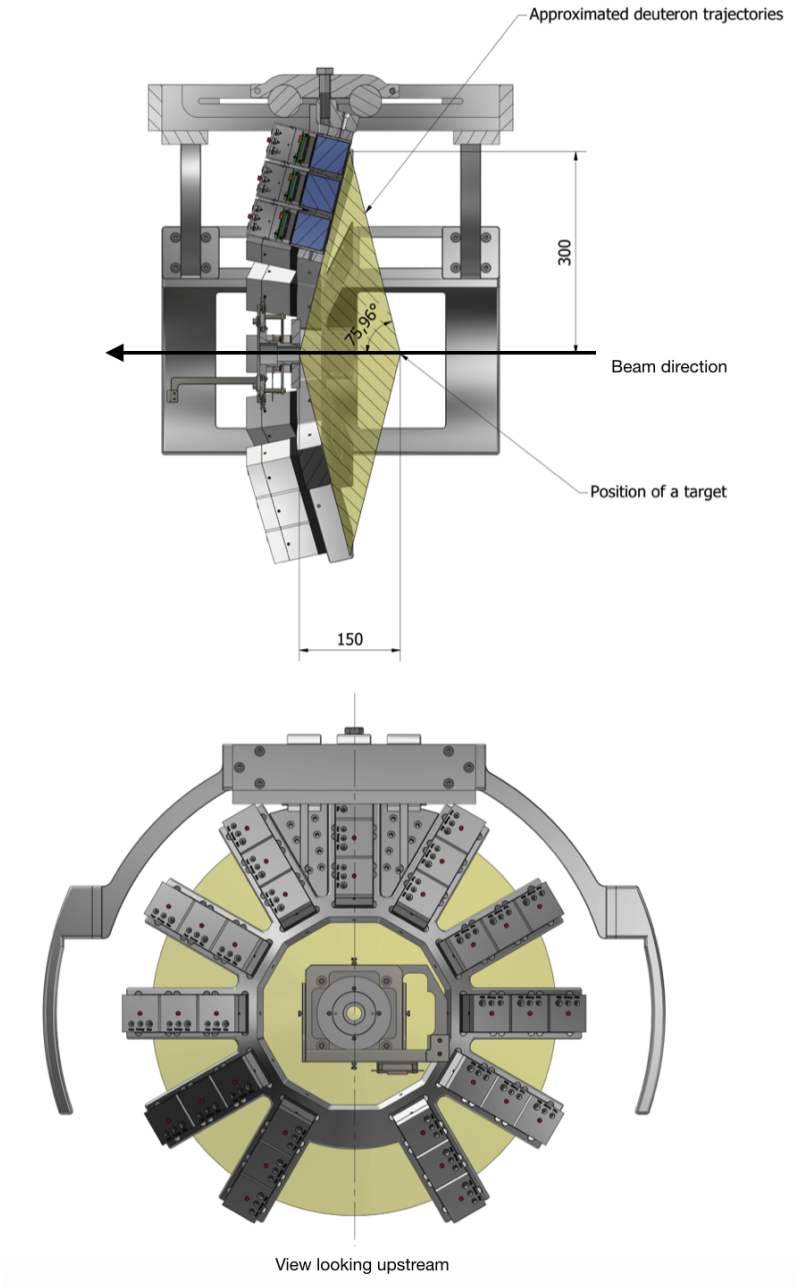

Figure A2: Drawings showing the $CeBr_3$ array situated inside the ISS bore, with 3 concentric rings of 11 individual crystals, read out by silicon photomultipliers. The detectors are situated approximately 150 mm downstream of the CD_2 target. Dimensions in mm.

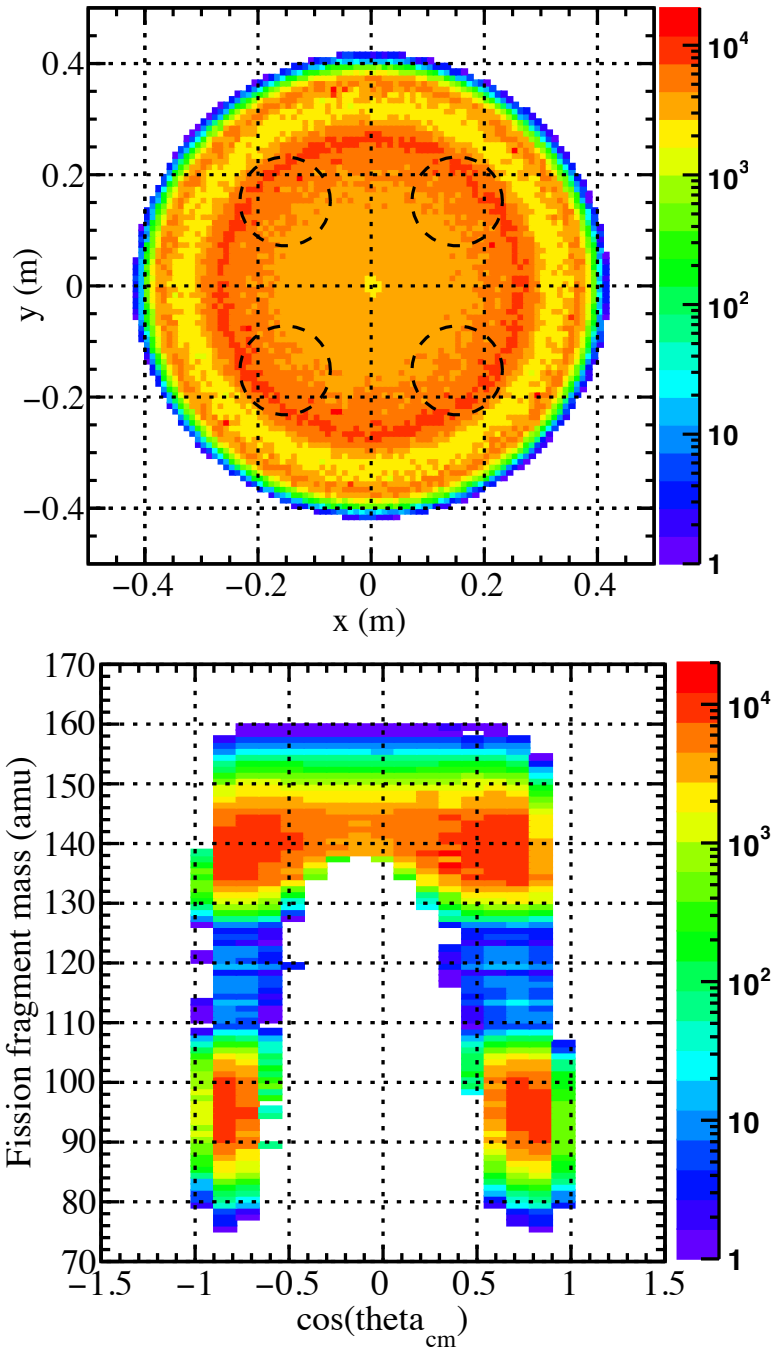

Figure A3: (Top) Spatial distribution of fission fragments from ^{235}U(d,pf) at 7 MeV/nucleon, shown at the downstream door of ISS, taking the solenoidal field mapping into account. The CD_2 target is positioned 55 mm downstream of the central point of the ISS vessel, and the detector apertures are situated 1.38 m from the target. The exit apertures of the vacuum vessel are represented by the dashed circles. The inner circular intensity region corresponds to heavy fragments, and the outer ring to light fragments. (Bottom) Coverage of the fission detector array, as a function of fission mass split and c.m. fission axis angle with respect to the beam axis.

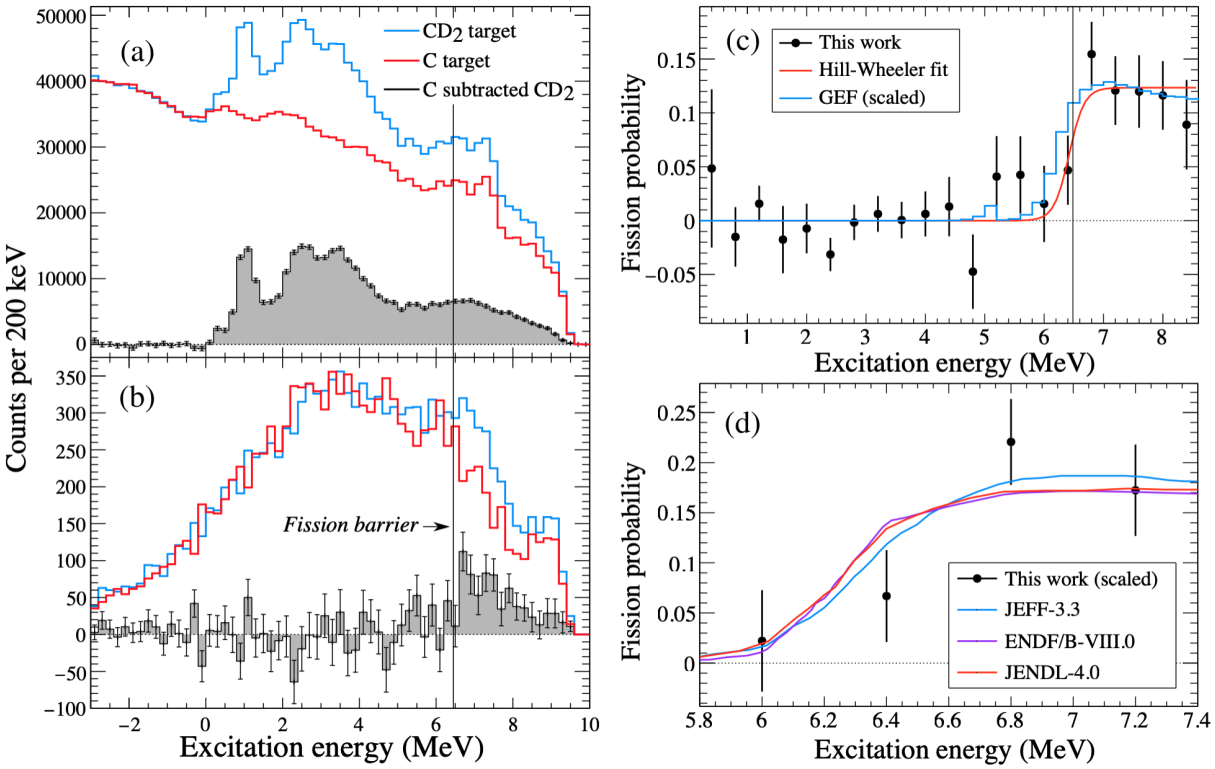

Figure A4: (a) and (b) Raw (d,p) and (d,pf) counts respectively from the ^{238}U(d,pf) reaction measurement with HELIOS at ANL. Data taken with CD_2 targets and ^{nat}C targets (scaled to the CD_2 data) are shown. (c) and (d) Experimental fission probability, as defined in Equation 1, compared to a GEF simulation [20] (the GEF result has been normalised to our data) and probabilities deduced from evaluated nuclear data libraries (JEFF-3.3, ENDF/B-VIII.0 and JENDL-4.0). Also shown is an empirical Hill-Wheeler fit to our measurement, corresponding to a barrier of 6.42(12) MeV. The vertical line denotes the known fission barrier, 6.46 MeV [21]. Figure adapted from Ref. [19].

Appendix B

DESCRIPTION OF THE PROPOSED EXPERIMENT

Part of the experiment	Design and manufacturing
ISOLDE Solenoidal Spectrometer	☐ To be used without any modification ☒ To be modified
Fission detectors, and bespoke rear door for ISS	☐ Standard equipment supplied by a manufacturer ☒ Collaboration responsible for the design and/or manufacturing

HAZARDS GENERATED BY THE EXPERIMENT
Additional hazard from flexible or transported equipment to the CERN site:

Domain	Hazards/Hazardous Activities		Description
Mechanical Safety	Pressure	☐	
	Vacuum	☐	
	Machine tools	☐	
	Mechanical energy (moving parts)	☐	
	Hot/Cold surfaces	☐	
Cryogenic Safety	Cryogenic fluid	☐	
Electrical Safety	Electrical equipment and installations	☐	
	High Voltage equipment	☒	4 kV
Chemical Safety	CMR (carcinogens, mutagens and toxic to reproduction)	☐	
	Toxic/Irritant	☐	
	Corrosive	☐	
	Oxidizing	☐	
	Flammable/Potentially explosive atmospheres	☐	
	Dangerous for the environment	☐	
Non-ionizing radiation Safety	Laser	☐	
	UV light	☐	
	Magnetic field	☒	2.3 T
Workplace	Excessive noise	☐	
	Working outside normal working hours	☐	
	Working at height (climbing platforms, etc.)	☐	
	Outdoor activities	☐	
Fire Safety	Ignition sources	☐	
	Combustible Materials	☐	
	Hot Work (e.g. welding, grinding)	☐	

Ionising radiation	Calibration sources	☒	α calibration source (open source)
			4236RP
			^{148}Gd, ^{239}Pu, ^{241}Am, ^{244}Cm
			1 kBq, 1 kBq, 1 kBq, 1 kBq
	Target materials		CD_2 (500 μg/cm^2) (Deuterated polyethelene)
			^{nat}C (500 μg/cm^2)
	Beam particle type		^{235}U
	Beam intensity		max. available (2.5×10^5 envisaged)
	Beam energy		max. available (7 MeV/nucleon envisaged)